UNIVERSITY OF PARDUBICE

FACULTY OF CHEMICAL TECHNOLOGY

Department of Biological and Biochemical Sciences

Jana Báčová

Assessment of cellular effects of nanomaterials

Thesis of the Doctoral Dissertation

Pardubice 2023

Study program: **Analytical chemistry**

Study field: **Analytical chemistry**

Author: **Mgr. Jana Báčová**

Supervisor: **doc. RNDr. Tomáš Roušar, Ph.D.**

Year of the defence **2023**

References

BÁČOVÁ, Jana. Assessment of cellular effects of nanomaterials. Pardubice, 2023. 136 pages. Dissertation thesis (PhD). University of Pardubice, Faculty of Chemical Technology, Department of Biological and Biochemical Sciences.
Supervisor: doc. RNDr. Tomáš Roušar, Ph.D.

Abstract

In recent years, the development and production of new nanomaterials, including nanoparticles, nanofibers, or nanotubes, have been increasing. However, nanomaterials can enter organisms due to their small size and induce biological effects in cells. In the last decade, attention has been given to studies investigating the biological effects of nanomaterials. Therefore, we aimed to study the cytotoxicity and biocompatibility of nanomaterials *in vitro*. We optimized the experimental conditions of TiO_2 P25 nanoparticle preparation for testing in human pulmonary A549 cells. We estimated TiO_2 P25 nanoparticle effects on dehydrogenase activity, glutathione levels, DNA fragmentation, and reactive oxygen species production. These nanoparticles did not cause any significant damage of cells in contrast to multi-walled carbon nanotubes.

We also estimated the biological effects of Al_2O_3, SiO_2, ZrO_2, TiO_2 and WO_3 fibers in comparison to nanoparticles of the same chemical composition. In general, our comprehensive study provided findings that inorganic fibers did not exhibit larger toxicity in A549 cells in comparison to nanoparticles. Then, we focused on the investigation of biological effects of Ti sheets and TiO_2 nanotubes modified by Atomic Layer Deposition technique using various cell lines. In addition, the surface modification by Atomic Layer Deposition significantly increased the biocompatibility of materials.

Keywords: TiO_2; fibers; nanoparticles; A549; dehydrogenase activity; glutathione; Atomic Layer Deposition.

Abstrakt

V posledních letech narůstá vývoj a výroba nových nanomateriálů, včetně nanočástic, nanovláken nebo nanotrubic. Nanomateriály však mohou vstupovat do organismů díky své malé velikosti a vyvolávat různé biologické účinky v buňkách. V posledním desetiletí je věnována značná pozornost studiím zkoumajícím biologické účinky těchto nanomateriálů. Proto jsme se zaměřili na studium cytotoxicity a biokompatibility nanomateriálů *in vitro.* Optimalizovali jsme experimentální podmínky přípravy nanočástic TiO_2 P25 pro testování na lidských plicních buňkách A549. Testovali jsme vliv nanočástic TiO_2 P25 na aktivitu dehydrogenáz, hladinu glutathionu, fragmentaci DNA a produkci reaktivních forem kyslíku. Tyto nanočástice nezpůsobily žádné významné poškození buněk na rozdíl od vícestěnných uhlíkových nanotrubic.

Také jsme hodnotili biologické účinky vláken Al_2O_3, SiO_2, ZrO_2, TiO_2 a WO_3 ve srovnání s nanočásticemi stejného chemického složení. Z naší komplexní studie vyplynulo, že anorganická vlákna nevykazovala větší toxicitu v buňkách A549 ve srovnání s nanočásticemi. Poté jsme se zaměřili na zkoumání biologických účinků titanových povrchů a TiO_2 nanotrubic modifikovaných technikou depozice atomárních vrstev s použitím různých buněčných linií. Dospěli jsme k závěru, že úprava povrchu pomocí depozice atomárních vrstev výrazně zvýšila biokompatibilitu těchto modifikovaných materiálů.

Klíčová slova: TiO_2; vlákna; nanočástice; A549; dehydrogenázová aktivita; glutathion; depozice atomárních vrstev.

Table of contents

1. Introduction

In recent years, the development and production of new nanomaterials, including nanoparticles, nanofibers, or nanotubes, have been increasing. Titanium dioxide nanoparticles are the most frequently used nanoparticles [1] that have been used in many applications, such as environmental protection and building engineering, agriculture, medicine, food and cosmetic industry [2-4]. After exposure, nanomaterials enter the human body through various ways, i.e., inhalation, injection, skin contact and absorption, causing occurrence of nanomaterials in organ tissues likely influencing their functions. Therefore, it is important to study and evaluate effects of nanomaterials in the human body [5].

The biological effects of nanomaterials, especially TiO_2 nanoparticles, in the human body has been investigated and discussed widely in the last decade. The initial phase of nanoparticle study includes testing their biological effects using human cell lines. One of the most used cell models for testing the biological effects of nanomaterials is the human pulmonary cell line A549 [6, 7]. The crystalline structure, particle size and coating can affect the surface charge, sedimentation, aggregation, and thus the action in cell models inducing different extent of toxicity [8]. In addition, due to high adsorption capacity and optical activity, nanoparticles have been also proven to influence cytotoxicity assays. The consequence is that a number of reports have been providing dissimilar results on detected level of toxicity of nanoparticles. Therefore, the assessment of nanoparticle effects *in vitro* needs a careful selection of the test systems [9, 10].

In addition to nanoparticles, the synthesis of polymeric and inorganic fibers with unique characteristics has been increasing in recent years. Fibers have exploited mainly for filtration media, tissue scaffolds or catalysts. The centrifugal spinning is a very modern and industrially robust technique for production of fibers. The unique inorganic fibers of different chemical composition, which have been recently synthesized by centrifugal spinning and brought to the market, have a promising potential for application in various fields [11]. On the other hand, due to increased human exposure to fibers, inhalation and their potential toxic effects in cells may occur [12].

Other types of nanomaterials show promising properties influencing cell adhesion, proliferation, and cell growth. Titanium and titanium alloys are representative of metallic biomaterials [13]. Nanomaterial modification can improve their surface properties and these nanomaterials have potential to find application in medicine, tissue engineering and implantology [14]. A recent example of this approach is titanium dioxide nanotubes modified using the Atomic Layer Deposition method. In this case, the surface of the material is modified with one or more layers of another material, for example, metal oxide, which is directly correlated with the improvement of metal surface properties [15]. Then, the biological integration and biocompatibility of various coated enriched substrates are evaluated using fibroblast and osteoblast-like cells.

2. Objectives of PhD study

1. To optimize and validate TiO_2 P25 nanoparticle preparation for biological testing in cultured pulmonary cells and to evaluate their biological effects.

2. To characterize the biological effects of nanomaterials of different shape and chemical composition, including inorganic nanoparticles vs. fibers and other TiO_2-derived nanomaterials in cultured pulmonary cells.

3. To estimate the effect of TiO_2 Atomic Layer Deposition coating of materials on their biocompatibility in cells *in vitro.*

3. Experimental part

3.1 Characterization and dispersion of TiO_2 P25 nanoparticles

TiO_2 P25 nanoparticles (anatase/rutile mixture, Product no. 718467, LOT MKCD 8503), were purchased from Sigma (USA). The size and morphology of TiO_2 P25 nanoparticles (TiO_2 P25 NPs) were characterized by a field-emission scanning electron microscope JSM 7500F (SEM, JEOL, Japan). X-ray diffraction (XRD) analysis was carried out using Panalytical Empyrean with Cu tube and Pixcel3D detector. Raman scattering spectrum of TiO2 P25, excited by a laser operating at 785 nm, was obtained using a Dimension P2 (Lambda Solution, USA). The topology of TiO_2 P25 surface was monitored on an atomic force microscope Dimension Icon (Bruker, Germany) according to the described procedure [16].

TiO_2 P25 stock solutions (10 $mg.mL^{-1}$) were prepared in distilled water. Different techniques were used to disperse TiO2 P25, i.e. (1) manual shaking by hand in a tube, (2) sonication using ultrasonic probe UP400S, 400 W, 24 kHz (Hielscher Ultrasonics GmbH, Germany), (3) FisherBrand FB15053H ultrasonic bath, 560 W (Fisher Scientific, UK), and (4) Ultraturrax® disperser T10 (IKA-Werke GmbH & Co. KG, Germany) equipped with a dispersion tool (S 10 D-7 G-KS-65) at 13,000 rpm. The dispersion of 100 $\mu g.mL^{-1}$ TiO_2 P25 was carried out for up to 60 min. Then, the mean hydrodynamic diameter DH was measured by 90Plus/BI-MAS Analyzer (Brookhaven Instruments Corp., USA) using dynamic light scattering (DLS).

In addition, TiO_2 P25 stock solutions (10 $mg.mL^{-1}$) were prepared in distilled water, 0.9% NaCl and Minimum Essential Medium (Sigma, USA) for cell culture w/wo 10% FBS (fetal bovine serum, Gibco, USA). The stock solutions were diluted to obtain the final concentration 100 $\mu g.mL^{-1}$ TiO_2 P25, vortexed for 1 min and dispersed in ultrasonic bath K2, 60 W, 33 kHz (Kraintek, Slovakia) for 10 min. Average particle size was determined by dynamic light scattering using a Zetasizer Nano ZS (Malvern PANalytical Ltd., United Kingdom).

3.2 Characterization of fibers

TiO_2, Al_2O_3, ZrO_2, SiO_2 and WO_3 fibers were synthesized using centrifugal spinning according to the protocol [11]. They were all supplied by the company Pardam Nano4Fibers, Ltd., as samples that represent their standard portfolio for inorganic fibers. Al_2O_3, ZrO_2 and TiO_2 P25 nanoparticles were supplied from Sigma (USA). SiO_2 nanoparticles and multiwalled carbon nanotubes (MWCNTs) were obtained from JRC Nanomaterials Repository. The resulting inorganic fibers kept their 3D bulky character, which was not suitable for the cell experiments. Thus, it was necessary to shorten the resulting fibers via ball milling using Spherical mill Retsch. The ball-milled fibers were significantly shortened but kept their fiber shape. Moreover, they became powder-like, which was more suitable for further handling (weighing, dispersing in water, exposure to cell line, etc.).

The morphological characterization of used materials was carried out using a field-emission scanning electron microscope (FE-SEM, JSM7500F, JEOL). Energy-dispersive X-ray spectroscopy (EDX) was used to analyze the composition of the samples using EDX detector (Oxford Instruments) integrated in SEM (TESCAN MIRA3-XMU) by employing accelerating voltage of 20 kV. The crystalline structure of the ball-milled fibers was characterized by an X-ray diffractometer (XRD, PANalytical Empyrean Cu Kα radiation).

3.3 Detection of endotoxin contamination

Nanomaterials were suspended in endotoxin-free water and diluted at 1 $mg.mL^{-1}$ concentration. Nanomaterials were vigorously vortexed, sonicated for 15 min and centrifuged (15,000g; 15 min). The endotoxin concentration was measured in the supernatant using the PyroGene™ Recombinant Factor C Assay (Lonza, Blackley, UK). According to manufacturer´s instructions, the presence of endotoxin in a sample was calculated using the standard curve and results were expressed as endotoxin concentration in $EU.mL^{-1}$.

3.4 A549 cell line

The A549 cell line was purchased from the American Type Culture Collection (ATCC No. CCL-185). The cells were cultured in Minimum Essential Medium with 10% (v/v) FBS, 2 $mmol.L^{-1}$ glutamine (Gibco, USA), 1 $mmol.L^{-1}$ pyruvate (Gibco, USA), 50 $\mu mol.L^{-1}$ penicillin/streptomycin solution (Gibco, USA) and maintained at 37 °C in a sterile humidified atmosphere of 5% CO_2. The cells were proven to be Mycoplasma-free and the origin of the cells was confirmed by STR analysis.

3.5 Other cell lines

Human osteoblast-like cells (MG-63, ATCC No. CRL-1427) and human lung fibroblast cells (WI-38, ATCC No. CCL-75) were cultured in Minimum Essential Medium with 10% (v/v) FBS and 50 $\mu mol.L^{-1}$ penicillin/streptomycin solution. Human neuroblastoma cells (SH-SY5Y, ATCC No. CRL-2266) were cultured in supplemented Dulbecco's modified Eagle's medium (Sigma, USA) with 15% (v/v) FBS and 50 $\mu mol.L^{-1}$ penicillin/streptomycin solution, followed by incubation in an atmosphere of 5% CO_2 at 37 °C. The cells were proven to be mycoplasma-free and the STR analysis confirmed the origin of all three cell lines.

3.6 Cell treatment with TiO_2 P25 nanoparticles

For *in vitro* experiments, stock solutions of 10 $mg.mL^{-1}$ TiO_2 P25 and MWCNTs were dispersed in culture medium w/wo FBS. Then, the stock solutions were vortexed for 1 min and sonicated for 10 min using ultrasonic bath K2. The working solutions were prepared by dilution in the culture medium without phenol red to obtain final concentrations of 1, 10, and 100 $\mu g.mL^{-1}$. A549 cells were seeded into 96-well plates at density of 10×10^3 cells per well. After 24 h of seeding, the cells were exposed to 1, 10, and 100 $\mu g.mL^{-1}$ TiO_2 P25. The cells were incubated with TiO_2 P25 at 37 °C in 5% CO_2 for 24 h. Unexposed cells were used as a negative control and MWCNTs were used as a positive control.

3.7 Cell treatment with fibers

Tested TiO_2, Al_2O_3, ZrO_2, SiO_2 and WO_3 fibers and nanoparticles were suspended in medium with 10% FBS to prepare stock solutions at concentration 1 $mg.mL^{-1}$. After sonication in ultrasonic bath K2 for 10 min to obtain an optimal dispersion, and agglomeration protection, the working solutions were prepared by the dilution in the culture medium with 10% FBS to final concentrations (1, 10 and 100 $\mu g.mL^{-1}$) to sustain the colloid stability of dispersed materials. This stability is predominantly ensured by protein presence, like in extracellular fluid. A549 cells were seeded into 96-well plates at density of 5×10^3 cells per well. After 24 h of seeding, the cells were exposed to the materials. The cells were incubated with materials for

24 or 48 h and the biological effect was tested. Untreated cells were used as a negative control. The multiwalled carbon nanotubes at concentration of 100 $\mu g.mL^{-1}$ were established as a positive control.

3.8 Cell cultivation on modified Ti sheets and TiO_2 nanotube layers

Different kinds of Ti sheets and TiO_2 nanotube (TNT) layers were modificated for testing of adhesion, growht and proliferation of different cells. Ti sheets and TNT layers and their surfaces Ti sheets with a native oxide layer (a-TiS), Ti sheets with a crystalline thermal oxide layer (c-TiS), and two kinds of TNT layers (prepared via electrochemical anodization) with a defined inner diameter of 12 and 15 nm were used as substrates (TNT 12 and TNT 15, respectively). A part of the Ti sheets and the TNT layers was additionally coated by thin 5 or 150 cycles of TiO_2 coatings using Atomic Layer Deposition (ALD) [17]. The surface morphology of all Ti sheets and TNT layers was characterized using a field-emission scanning electron microscopy (FE-SEM, JEOL JSM 7500F).

All Ti sheets and TNT layers were sterilized in 70% ethanol for 30 min, washed with deionized water and dried. Then, the samples were placed into eight-well chamber slides. Briefly, 200 µL of a suspension of MG-63, WI-38, and SH-SY5Y cells with a density of 7×10^3, 2×10^4, and 2×10^4 per well, respectively, was added into each well of a chamber slide and the cells were cultured for 24 h.

3.9 Measurement of dehydrogenase activity

The cell viability was assessed using WST-1 test (Sigma, USA), which detects the activity of mitochondrial dehydrogenases. After incubation with nanomaterials, WST-1 reagent was added to each well according to the manufacturer's instructions. After 1 h, the change of absorbance was measured at the wavelength of 440 nm using SPARK microplate reader (Tecan, Austria). The dehydrogenase activity was expressed as the percentage of total cellular dehydrogenases activity relative to that in control cells (control = 100%).

3.10 Measurement of glutathione levels

The glutathione (GSH) levels were measured using an optimized monochlorobimane assay [18]. The working solution of monochlorobimane (MCB, Sigma, USA) was prepared fresh at the time of analysis by dilution in Dulbecco's phosphate buffer (Sigma, USA) and tempered at 37 °C. After the treatment with nanomaterials, MCB solution was added to the cells in 96-well plates and the measurement started immediately. The final concentration of MCB in a well was 40 $\mu mol.L^{-1}$. The fluorescence intensity (Ex/Em = 394/490 nm) was measured kinetically for 20 min using SPARK microplate reader (Tecan, Austria). The fluorescence was expressed as the slope of a fluorescence change over time. GSH levels were expressed as the percentage relative to GSH levels in control cells (control = 100%).

3.11 Detection of DNA fragmentation and reactive oxygen species

To measure nuclear condensation and fragmentation in intact cells, we used a fluorescence dye: Hoechst 33258 (H33258) [19]. After treatment with tested nanomaterials for 24 h, the cells were incubated with H33258 and spectrofluorometric measurement was performed using SPARK microplate reader (Tecan, Austria) while incubated at 37 °C. After

background subtraction, the fluorescence signal was presented in Relative Fluorescence Units (RFU) as mean ± SEM.

Chloromethyl-2',7'-dichlorodihydrofluorescein diacetate (CM-H_2DCFDA) was used as an intracellular probe to detect reactive oxygen species (ROS) production [20]. After 24 h incubation with TiO_2 P25 and MWCNTs, CM-H_2DCFDA was added to cells to be loaded for 90 min. The final concentration of CM-H_2DCFDA in a well was 5 μmol.L^{-1}. The fluorescence was measured for 60 min using SPARK microplate reader (Tecan, Austria). The ROS levels were expressed as the percentage relative to ROS levels in control cells (= 100%).

All experiments were repeated at least three times independently. Three replicates were used in each independent experiment. The results are expressed as a mean ± S.D. Statistical analysis was performed using OriginPro 9.0.0 (OriginLab, USA). The analysis of variance followed by Bonferroni or Tukey post-test was used to perform the mean comparison at significance level *$p=0.05$ (*, $p < 0.05$, **, $p < 0.01$, ***, $p < 0.001$)*.

3.12 Fluorescence staining and cell counting

To visualize the cells, we used two fluorescence probes: Hoechst 33258 (Sigma, USA) to stain the cell nucleus and phalloidin-fluorescein isothiocyanate (FITC) (Sigma, USA) to stain actin filaments in cells. After 24 h of seeding, the cultured cells were fixed by 3.7% formaldehyde (5 min; 37 °C; dark) and permeabilized by 0.1% Triton X 100 (15 min; 37 °C; dark). Then, 100 μL of phalloidin-FITC was incubated for 30 min at 37 °C to obtain a final concentration of 1 μmol.L^{-1} phalloidin-FITC in a well. After incubation, 10 μL of Hoechst 33258 solution was added to the cells for 10 min. The final concentration of Hoechst 33258 in a well was 2 μg.mL^{-1}. After the loading process, the cells were washed two times with phosphate buffer. The actin filaments (FITC filter, 480/30 nm) and cell nuclei (DAPI filter, 375/ 28 nm) were observed with an Eclipse 80i fluorescence microscope (Nikon, Japan). The number of cells grown on the surface was counted minimally from 20 fields of view using NIS-Elements AR (Nikon, Japan). All experiments were repeated 3−5 times independently. The number of cell nuclei was related to 1 mm^2 and expressed as mean ± standard error of mean (SEM).

4. Published results

4.1 Characterization and dispersion of TiO_2 P25 nanoparticles

We characterized shape and size of commercially available TiO_2 P25 NPs using scanning electron microscopy. We found that TiO_2 P25 were supplied in a form of agglomerates with an average size over 1 μm in maximal dimension. Those agglomerates were composed of primary particles with size 30±10 nm but the primary particles were obviously interconnected by solid bridges to each other. The phase composition of TiO_2 P25 was analyzed by X-ray diffraction analysis. The sample of TiO_2 P25 consisted of 90.4% (wt) of anatase (ICDD:00–021-1272) and 9.6% (wt) of rutile (ICDD:00–021-1276) phases. The crystallite size for anatase phase of ≈ 27 nm was determined by Rietveld method.

A proper dispersion of TiO_2 P25, i.e., a separation of aggregates into ideally a mixture of well-separated single particles, is a crucial point for assessment of their biological effects. Thus, the rate of dispersion of TiO_2 P25 in distilled water was tested using four techniques. In addition to the hydrodynamic diameter measurement of TiO_2 P25 dispersed for 40 min

(Fig. 1A), we tested the effect on duration of dispersion (Fig. 1B). Our results showed that the maximal rate of dispersion of TiO_2 P25 in distilled water was found in nanoparticles dispersed using ultrasonic probe and bath. The use of both techniques, however, provided also fractions of dispersed nanoparticles being larger than 200 nm (Fig. 1A). Our results on the extent of TiO_2 P25 dispersion in time (Fig. 1B) showed that the effective hydrodynamic diameter remained predominantly stable. The duration to obtain the maximal rate of dispersion was determined to be at least 10 min.

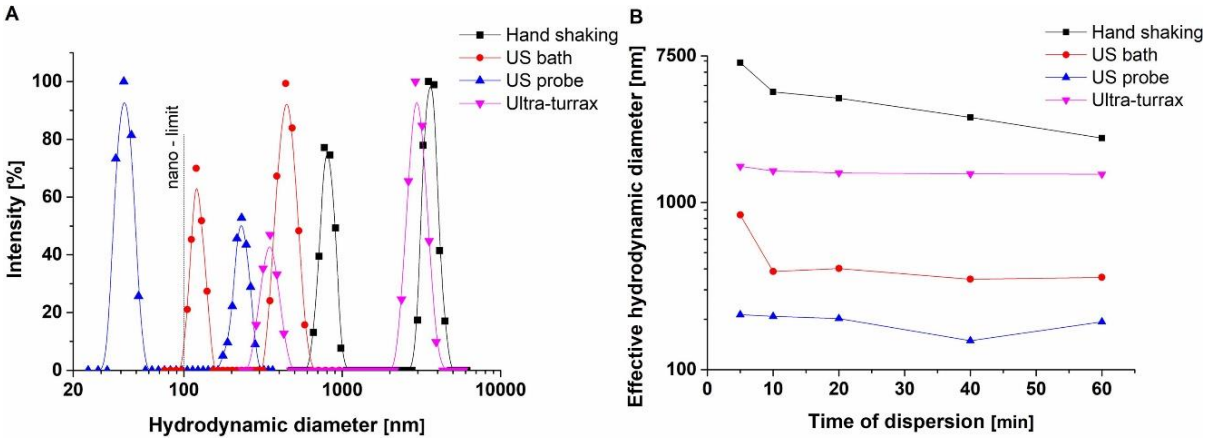

Fig. 1. Results of dispersion of TiO_2 P25 in distilled water (100 µg.mL^{-1}) Using four dispersion techniques: hand shaking, ultrasonic (= US) bath, US probe and Ultra-turrax. The particle size distribution was measured after 40 min of dispersion (A) and after dispersion for 5-60 min (B).

Generally, the testing of nanomaterials in cells, however, requires a use of culture media containing all necessary ingredients to ensure the cell growth and proliferation. Thus, we tested the behavior of TiO_2 P25 in distilled water in comparison to the dispersion stability in saline solution and Minimum Essential Medium for cell culture with or without addition of 10% fetal bovine serum. Thus, we used the dispersion of TiO_2 P25 nanoparticles using ultrasonic bath for 10 min. We determined the relation of obtained extent of TiO_2 P25 dispersion and used environment (Fig. 2). The final evaluation of our data on dispersion of TiO_2 P25 provided essential information on necessity of FBS presence in assessment of biological effects of TiO_2 P25 in cell culture media to ensure as large as possible dispersion. We conclude that a number of factors have been influencing the accomplishment of proper TiO_2 P25 dispersion, i.e., dispersion technique, duration, ingredients in the cell culture medium and also the interval between preparation of TiO_2 P25 suspension and addition to cultured cells. Thus, in all following experiments, we prepared TiO_2 P25 suspensions using sonication in ultrasonic bath (10 min) in cell culture medium with FBS ensuring the colloidal stability.

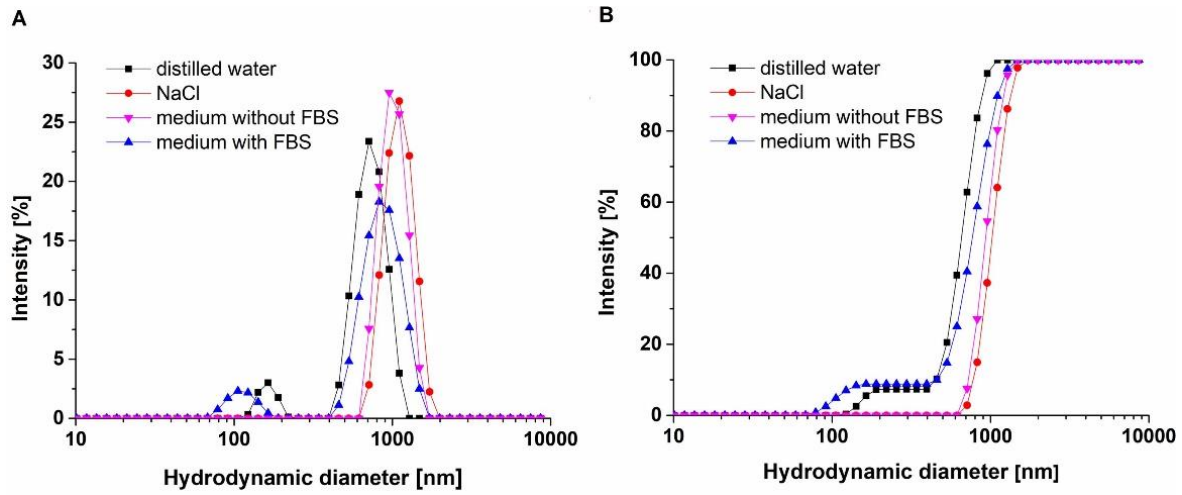

Fig. 2. Results of TiO_2 P25 size distribution (100 µg.mL^{-1}) in distilled water, 0.9% NaCl, cell culture medium w/wo 10% fetal bovine serum (FBS) for 10 min using ultrasonic bath. Data are presented as intensity distribution (A) and cumulative intensity (B) of TiO_2 P25 size.

4.2 Effects of fetal bovine serum in TiO_2 P25 treatment of A549 cells

We tested TiO_2 P25 for potential endotoxin contamination. We found that the concentration of endotoxin in the sample occurred under the detection limit of the assay (<0.005 EU.mL^{-1}). Then, we estimated the influence of the fetal bovine serum presence on TiO_2 P25-induced biological effects. A549 cells were treated with 0–100 µg.mL^{-1} TiO_2 P25 w/wo FBS. After 24 h, we estimated an effect of TiO_2 P25 on the cell viability and glutathione levels measured using the WST-1 test and monochlorobimane, respectively (Tab. 1).

Tab. 1. Dehydrogenase activity and glutathione levels were assayed in A549 cells treated with 0-100 µg.mL^{-1} TiO_2 P25 in culture medium w/wo fetal bovine serum (FBS) for 24 h. The results are expressed as mean ± S.D. (*p < 0.001*, compared to untreated cells).

Cell culture	TiO_2 P25 [µg.mL^{-1}]	Dehydrogenase activity	Glutathione level
without FBS	0	100 ± 3%	100 ± 3%
	1	99 ± 5%	100 ± 5%
	10	101 ± 4%	98 ± 5%
	100	97 ± 4%	85 ± 7% *(p < 0.001)*
with FBS	0	100 ± 3%	100 ± 4%
	1	97 ± 5%	104 ± 6%
	10	98 ± 8%	91 ± 4% *(p < 0.001)*
	100	97 ± 9%	87 ± 4% *(p < 0.001)*

In A549 cells incubated with or without FBS, we found that none of the tested TiO_2 P25 concentrations affected cellular dehydrogenase activity significantly in comparison to untreated cells. A slight decrease of dehydrogenase activity to 97 ± 4% was detected only in 100 µg.mL^{-1} TiO_2 P25 treated A549 cells with FBS. Measurement of glutathione levels, as an essential intracellular antioxidant, detected a significant glutathione depletion in 100 µg.mL^{-1} TiO_2 P25 treated A549 cells grown both with and without FBS. In addition, mild, but significant glutathione depletion was observed in A549 cells with FBS exposed to 10 µg.mL^{-1} TiO_2 P25.

4.3 Estimation of TiO_2 P25 effects in A549 cells

We used three additional methods for characterizing the TiO_2 P25 effects in A549 cells in more detail, i.e., determination of nuclear condensation and fragmentation, ROS production and assessment of cell morphology (Fig. 4). After 24 h, we found that none of tested TiO_2 P25 concentrations induced significant nuclear condensation and fragmentation in comparison to untreated cells. Only a mild increase of DNA condensation was found with 100 $\mu g.mL^{-1}$ TiO_2 P25, implying that TiO_2 P25 treatment did not cause an induction of apoptotic cell death. On the other hand, a significant increase of nuclear condensation and fragmentation was detected in MWCNTs treated A549 cells (Fig. 4A).

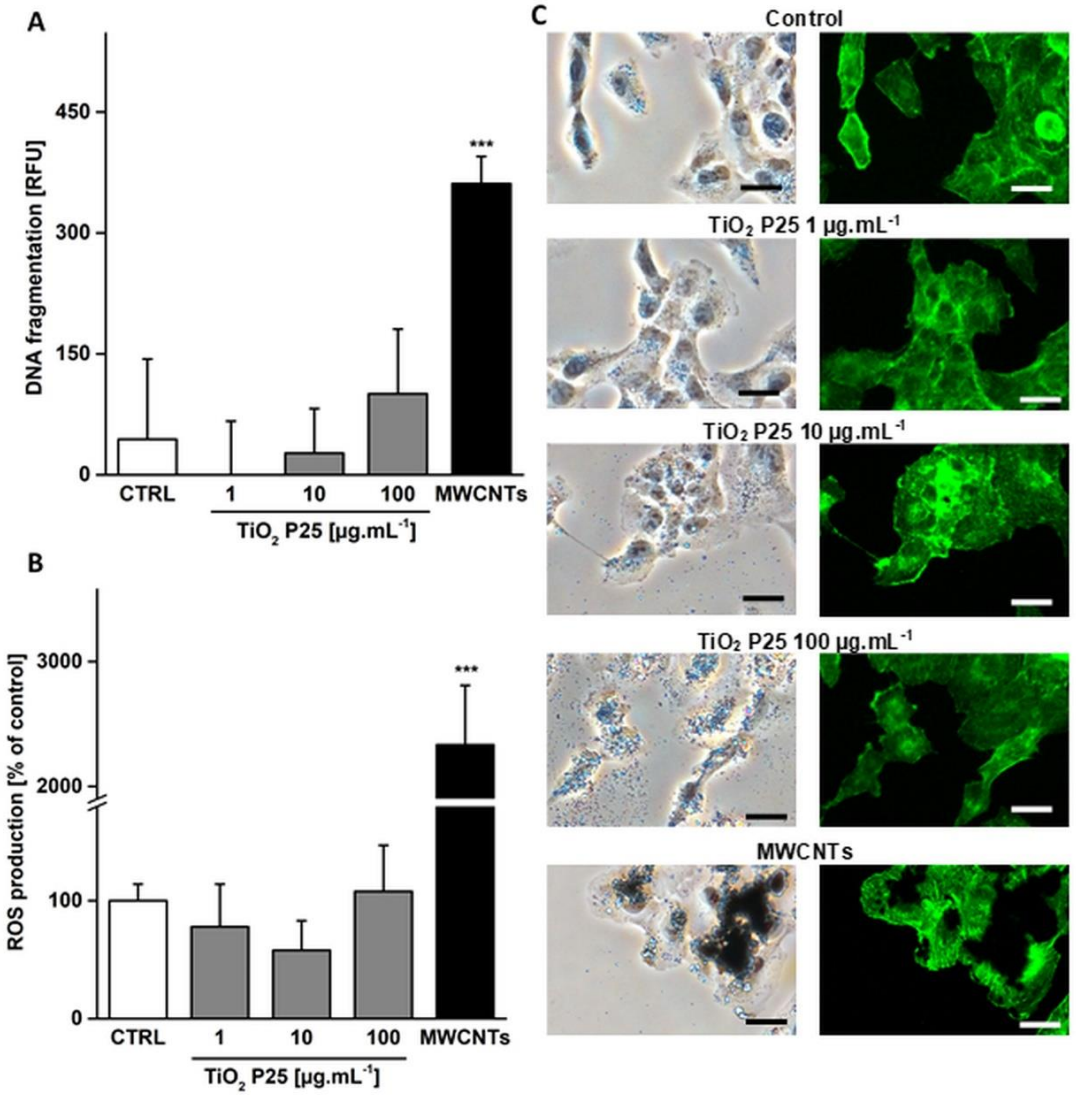

Fig. 4: Estimation of TiO_2 P25 effects in A549 cells. A549 cells were treated with TiO_2 P25 (0-100 $\mu g.mL^{-1}$) and MWCNTs (100 $\mu g.mL^{-1}$) with fetal bovine serum for 24 h. (A) nuclear condensation and fragmentation, (B) Reactive oxygen species (ROS) production and (C) A549 cells morphology (scale bar = 10 µm) were estimated. The results are expressed as mean ± S.D. (*, $p < 0.001$, compared to untreated cells).**

To observe any induction of an oxidative stress after TiO_2 P25 treatment in A549 cells, we investigated the production of reactive oxygen species. After 24 h of incubation, we did not observe any significant induction of ROS production in tested TiO_2 P25 in comparison to untreated A549 cells (Fig. 4B). MWCNTs treatment, however, induced significant increase of ROS production. Fluorescence staining of actin filaments and phase contrast microscopy

were used for a visual evaluation of TiO_2 P25-treated A549 cells (Fig. 4C). Typical epithelial morphology was found in both untreated and TiO_2 P25-treated A549 cells, showing no significant effect of TiO_2 P25 treatment compared to MWCNTs. Finally, according to the outcomes of all experiments using different methods for characterizing the effect of TiO_2 P25 in A549, we concluded that TiO_2 P25 treatment induced no significant cell impairment.

4.4 Effect of fibers and nanoparticles on dehydrogenase activity in A549 cells

The aim of our study was to evaluate the biological effects of various materials including fibers and nanoparticles differing in their shape and chemical composition. Fig. 5 shows the SEM images of the ball-milled inorganic fibers used for cell treatment. As one can see from these images, the fibers did not crack longitudinally (along their bodies), but across their bodies. So, at the end, they became shorter than the as-produced fibers, but not necessarily smaller in diameter.

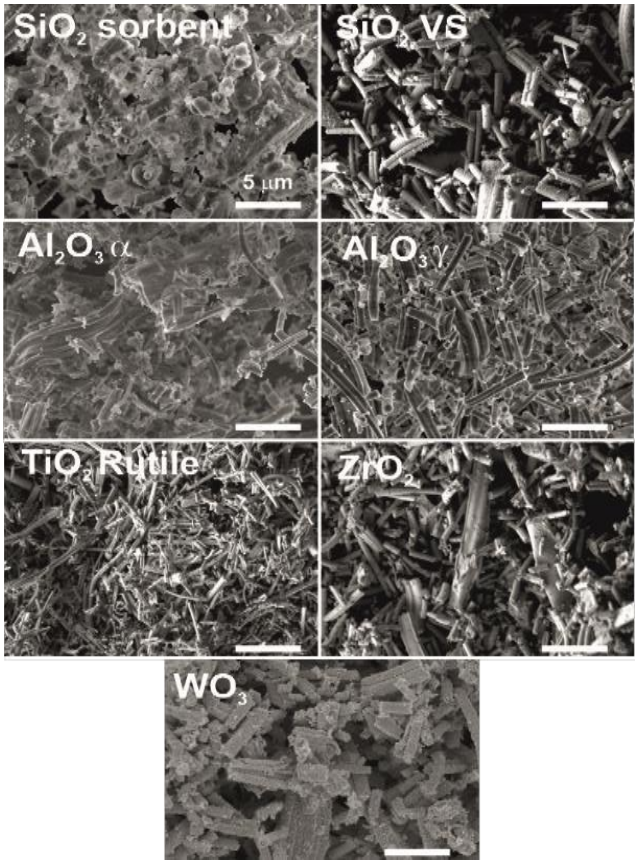

Fig. 5. SEM images of the ball-milled inorganic fibers used for biological testing (scale bars represent 5 μm).

We found that the concentration of endotoxin in all fibers, nanoparticles and MWCNTs occurred at the detection limit of the assay. Thus, all tested nanomaterials were proven to be endotoxin free. Then, we estimated the effect of the materials on the cell viability using the WST-1 test. Our results (Fig. 6A) showed that 1 and 10 $\mu g.mL^{-1}$ concentrations of all tested materials except 10 $\mu g.mL^{-1}$ WO_3 fibers did not induce a significant decrease in cellular dehydrogenase activity after 24 h of incubation. On the other hand, 24 h of treatment with 100 $\mu g.mL^{-1}$ Al_2O_3 α, TiO_2 rutile or WO_3 fibers and 100 $\mu g\ mL^{-1}$ Al_2O_3, TiO_2 P25 or WO_3 NPs caused a significant decrease in dehydrogenase activity. The largest impairment was found in MWCNTs and Al_2O_3 α fiber treated A549 cells, where the dehydrogenase activity was

reduced to 73 ± 5% *($p < 0.001$)* and 83 ± 7% *($p < 0.001$),* respectively, compared to untreated cells.

After 48 h, we found that the cell damage predominantly deepened (Fig. 6A) in cells treated with 100 μg.mL^{-1} concentration of some materials in comparison to 24 h. In addition, we detected a significant impairment in cells exposed also to 10 μg.mL^{-1} SiO_2 VS fibers. Although the significant cell damage was induced by most of the tested materials, none of them caused cellular impairment at the extent comparable to MWCNTs. We concluded that according to the outcomes from the WST-1 test, the largest cellular impairment was caused by Al_2O_3- and TiO_2-derived materials. However, the cell damage was predominantly detectable only at the highest tested concentration and none of the tested materials induced cell damage comparable to MWCNTs. No significant changes of cell metabolism were observed in A549 cells treated with ZrO_2-derived materials. Importantly, no significant difference in induction of cell impairment was found after comparison of dehydrogenase activities of cells treated with fibers and NPs of the same chemical composition.

4.5 Effect of fibers and nanoparticles on glutathione levels in A549 cells

In addition to the WST-1 test, we measured the cellular levels of glutathione, as the essential intracellular antioxidant. The results on GSH levels (Fig. 6B) showed that there was a positive correlation with the findings observed using the WST-1 test. After 24 h of treatment, a significant glutathione depletion was found in A549 cells treated with 100 μg.mL^{-1} Al_2O_3 α, Al_2O_3 γ and TiO_2 rutile fibers and with 100 μg.mL^{-1} TiO_2 P25 in comparison with untreated cells. The largest GSH depletion was found in MWCNTs and TiO_2 rutile fibers treated cells where GSH levels were reduced to 78 ± 12% *($p < 0.001$)* and 80 ± 7% *($p < 0.001$)*, respectively, compared to untreated cells. At 24 h, no significant effect on GSH levels was observed after treatment with SiO_2, ZrO_2 or WO_3 fibers and with Al_2O_3, SiO_2, ZrO_2 or WO_3 NPs. After 48 h of treatment, GSH levels remained depleted in A549 cells treated with all materials causing GSH depletion after 24 h (Fig. 6B).

In addition, significant GSH depletion was detected in A549 cells exposed to 100 μg.mL^{-1} SiO_2 VS and WO_3 fibers. Although significant, the negative biological effect of SiO_2 VS and WO_3 fibers was, however, very mild because the incubation with both materials reduced the GSH levels only by 10% compared to untreated cells. The largest GSH depletion was found again in MWCNTs treated A549 cells (74 ± 11%, $p < 0.001$, vs. untreated cells). The GSH concentration after incubation with 100 μg.mL^{-1} Al_2O_3 α, Al_2O_3 γ and TiO_2 rutile fibers or with 100 μg.mL^{-1} TiO_2 P25 NPs occurred between 77% and 83% of GSH levels compared to untreated cells. In summary and in accordance with the outcomes from the WST-1 test, the measurements of GSH levels in A549 cells treated with the tested materials did not show any significant relation of observed toxicity to the shape of a nanomaterial at similar concentrations. Only Al_2O_3 and WO_3 fibers at the highest concentration of 100 μg.mL^{-1} seemed to exhibit a larger capability to deplete glutathione levels than nanoparticles of the same chemical composition.

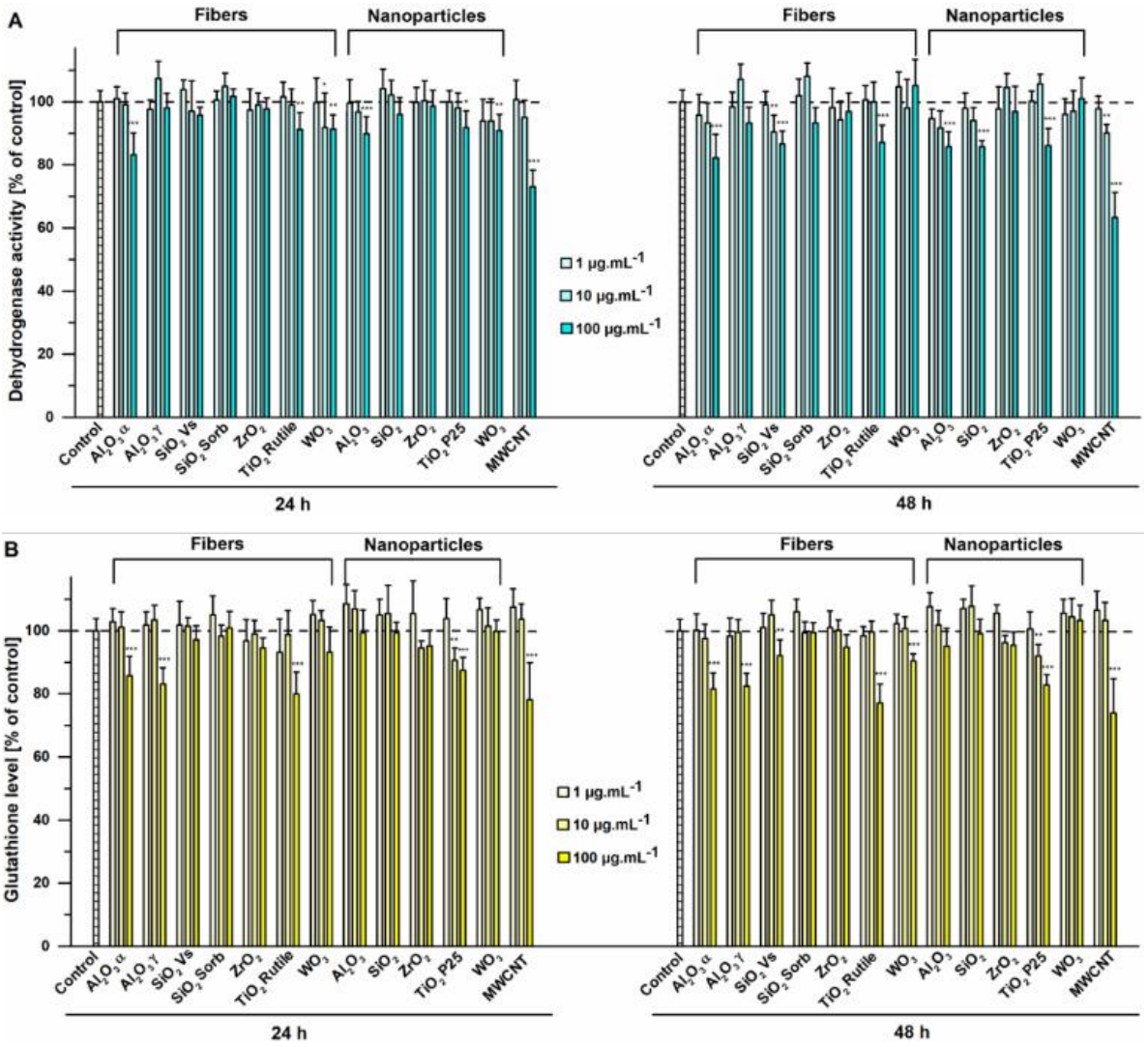

Fig. 6. Effect of fibers and nanoparticles on dehydrogenase activity (A) and glutathione levels (B) in A549 cells after 24 and 48 h of treatment. Data are expressed as means ± SD (n=12). *, *p < 0.05*, **, *p < 0.01*, *, *p < 0.001* vs. untreated control cells.**

4.6 Effects of TiO_2 ALD modified surfaces on cell growth

Cell behavior, i.e., adhesion and growth, was evaluated in the response to uncoated and ALD TiO_2-coated surfaces of Ti sheets and TNT layers using fibroblast WI-38 cell line (i.e., counting of cells to quantitate their occurrence per mm^2). The diameters of TNT layers were chosen ~12 nm, TNT 12, and ~15 nm, TNT 15 (Fig. 7). In general, increased hydrophilicity leads to enhanced cell growth [21]. Therefore, increased WI-38 cell growth on Ti sheets and TNT layers after 5c ALD TiO_2 can be also ascribed to the enhanced wettability of the surfaces that induced WI-38 cell adhesion and growth (Fig. 8). Here, using a much lower number of ALD cycles, the resulting biomaterial exhibited beneficial properties of both the original substrate (Ti sheets and TNT layers) and the additional ALD TiO_2 coating. By this effort, the original surface of a-TiS and cTiS was preserved.

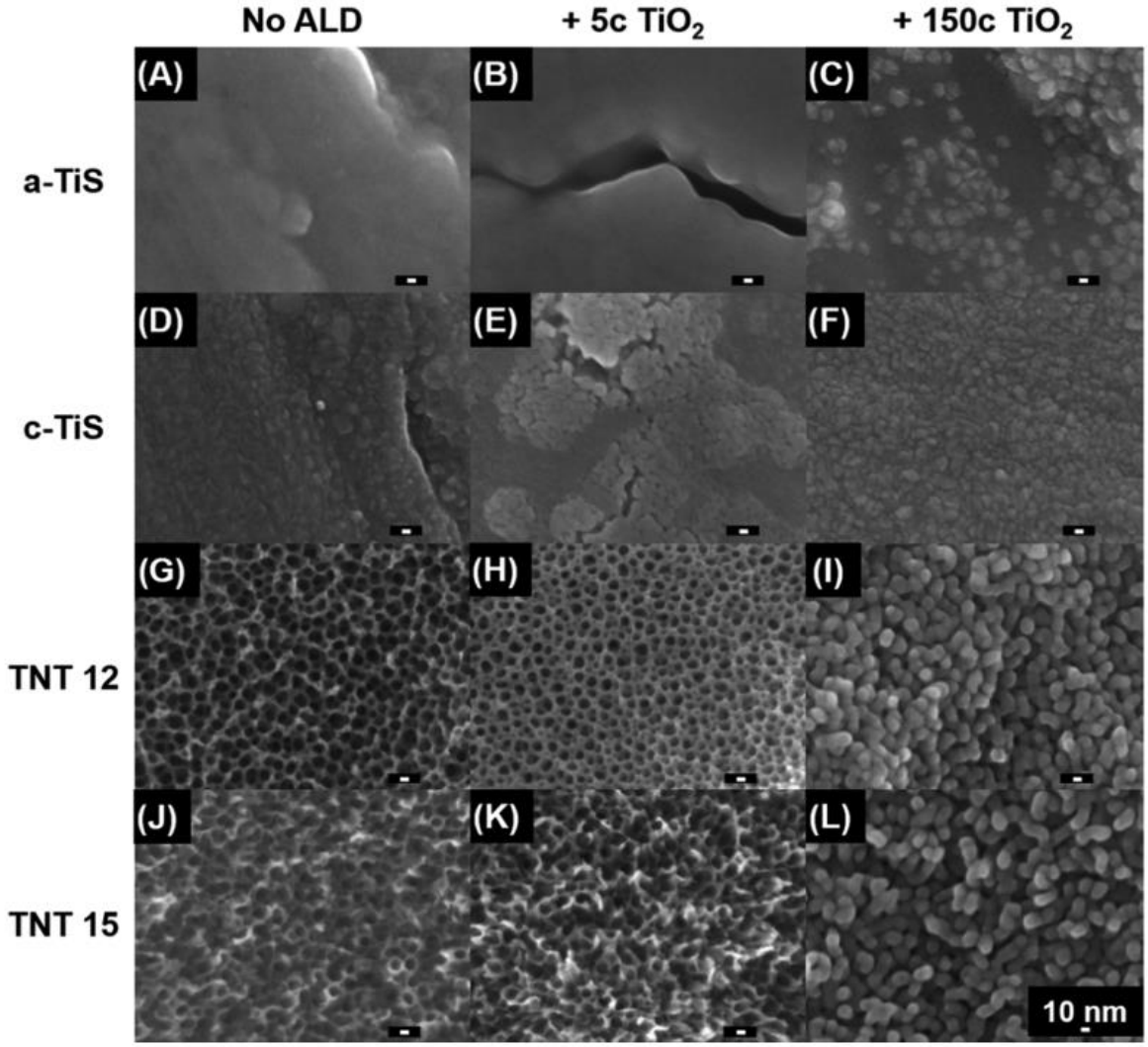

Fig. 7. SEM top-view images of (A, B, C) Ti sheets with a native amorphous oxide layer (a-TiS), (D, E, F) Ti sheets with a crystalline thermal oxide layer (c-TiS), (G, H, I) TiO_2 nanotube (TNT) layers with an inner diameter of ~12 nm, and (J, K, L) TNT layers with an inner diameter of ~15 nm. The left column shows uncoated samples, the middle column + ALD 5c TiO_2, and the right column + ALD 150c TiO_2; (ALD=Atomic Layer Deposition).

Moreover, the additional ALD TiO_2 coating is crystalline after 150 ALD TiO_2 cycles compared to the amorphous TiO_2 coating after 5 ALD TiO_2 cycles. The crystalline status of TiO_2 is a crucial factor affecting cell behavior. In general, the differences in cell behavior on amorphous and crystalline TiO_2 surfaces depend on the cell type (i.e., primary cells versus cell lines) and different methods employed to assess cellular activities [22]. Here, the WI-38 cell growth was increased on Ti sheets and TNT layers after coating by 150 ALD TiO_2 cycles compared to their uncoated counterparts, but it was not so high compared to the WI-38 cell growth on Ti sheets and TNT layers coated by 5 ALD TiO_2 cycles. Like the thin ALD TiO_2 coating (after 5 ALD TiO_2 cycles), the significantly thicker additional ALD TiO_2 coating (after 150 ALD TiO_2 cycles) covers the surface contaminants on Ti sheets and TNT layers. This itself influences the increased cell growth and the additional ALD TiO_2 coating also protects TNT layers from water annealing. However, except the change in crystallinity, coating by 150 ALD TiO_2 cycles was accompanied by significant morphological changes of Ti sheets and TNT layers. The surface of Ti sheets and TNT layers after 150 ALD TiO_2 cycles was less favored for cell growth compared to the surface after 5 ALD TiO_2 cycles, where the morphology of the original TNT layers was preserved. This comparison between the results obtained for 5 and

150 ALD TiO_2 cycles clearly points out that for a given substrate, the composition of the surface compared to the surface roughness has a more important effect on cell growth.

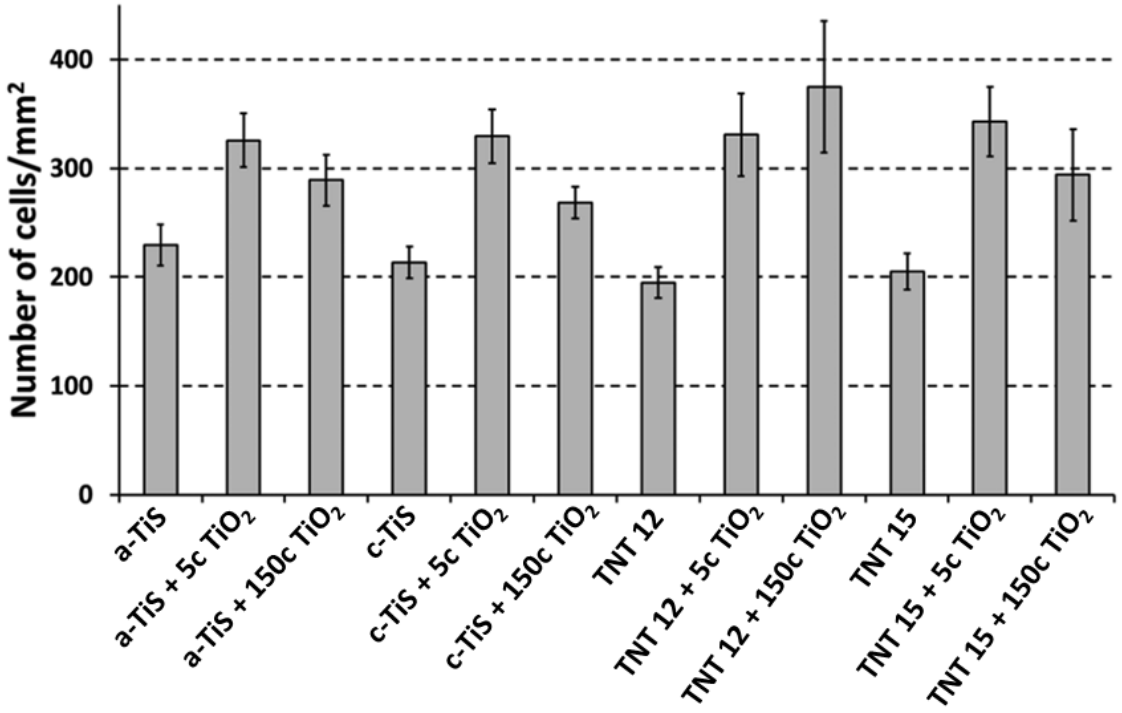

Fig. 8. Density of WI-38 cells grown for 24 h on uncoated and ALD-coated (5c and 150c TiO_2) Ti sheets with a native oxide layer (a-TiS), Ti sheets with a crystalline thermal oxide layer (c-TiS), and TiO_2 nanotube (TNT) layers with inner diameters of 12 and 15 nm (TNT 12 and TNT 15). Data are presented as mean ± SEM.

At last, the cell growth of SH-SY5Y neuroblasts and MG-63 osteoblasts on uncoated and ALD TiO_2-coated TNT layers was evaluated. Those cell lines with a different origin and morphology (SH-SY5Y have a stellar shape, while MG-63 have a round shape) were chosen to compare the outcomes from experiments with WI-38 cells of an elongated shape. Only uncoated and ALD 5c TiO2-coated TNT layers were further studied. MG-63 osteoblast and SH-SY5Y neuroblast cell growth was increased by >30% on TNT layers coated by 5 ALD TiO_2 cycles compared to their uncoated counterparts (Fig. 9).

This novel ALD-based approach offers three distinct advantages: (1) The shown Ti sheets and TNT layers coated by additional thin ALD TiO_2 coating (nominal thickness of approx. 0.3 nm) retain their original structure. This is especially demanded for TNT layers with their unique morphology. (2) A thin ALD TiO_2 coating protects the TNT layers from crystallization and shape change due to water annealing and prevents contaminants (naturally occurring on the surface of all materials) from being in direct contact with cells. (3) The risk of delamination of the additional ALD TiO_2 coating is avoided due to the nature of the ALD process creating strong chemical bonds between substrates and coatings. The results presented here pave a way for the ALD modification of various TiO_2-based and other oxide substrates to increase their biocompatibility and promote cell growth.

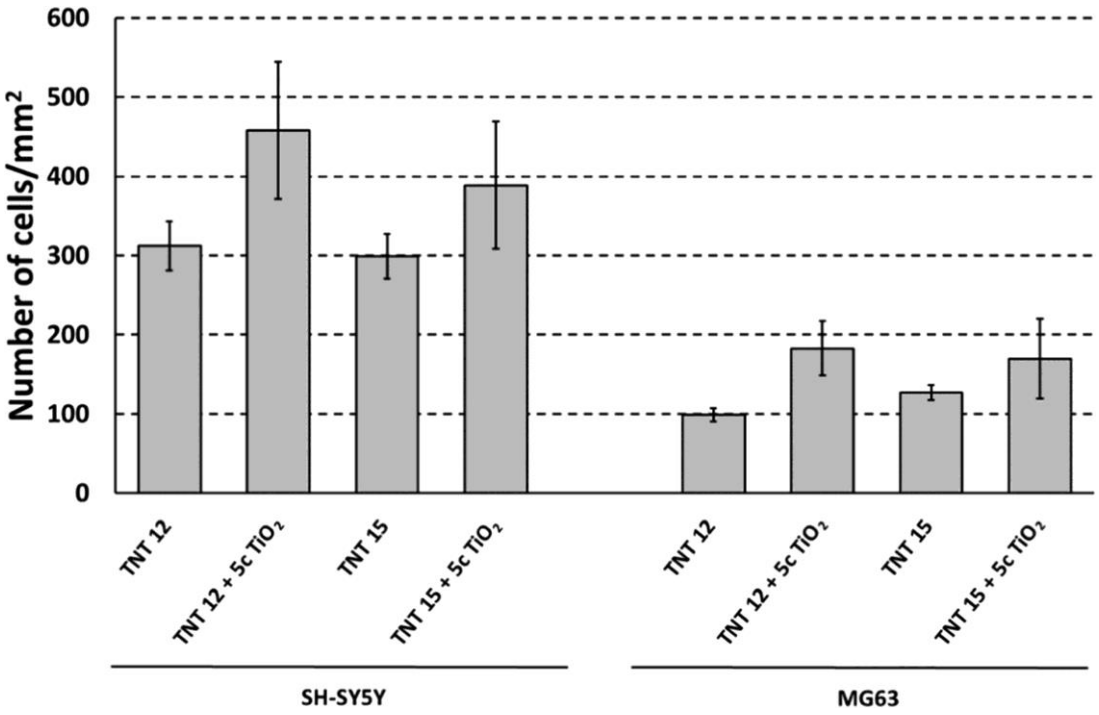

Fig. 9. Density of SH-SY5Y and MG-63 cells grown for 24 h on uncoated and ALD-coated (5c TiO_2) TiO_2 nanotube (TNT) layers with inner diameters of 12 and 15 nm (TNT 12 and TNT 15, respectively). Data are presented as mean ± SEM.

5. Conclusion

Herein, three topical studies investigating the biological effects of commercially available or newly synthesized nanomaterials on cells were presented. Firstly, we optimized and validated preparation of TiO_2 P25 nanoparticles for biological testing in pulmonary cells A549. We found that TiO_2 P25 nanoparticles, in contrast to MWCNTs, were not capable of inducing significant cell damage. Our results can provide benefits for other researchers using TiO_2 P25 nanoparticles as a benchmark material in estimating pulmonary toxicity in A549 cells.

In addition, we evaluated the cellular toxicity of unique inorganic fibers, which have been recently synthesized and brought to the market. We found that the tested fibers of different chemical composition caused no or very mild cell impairment in pulmonary A549 cells treated only with the highest concentration compared to nanoparticles of the same chemical composition.

Finally, we estimated the effect of TiO_2 Atomic Layer Deposition coating of materials on their biocompatibility in cells. Our results showed that coating of these surfaces with only 5 TiO_2 cycles using Atomic Layer Deposition significantly improved cell growth on the surfaces. Atomic Layer Deposition represents a promising way for modification of various TiO_2-based and other oxide substrates to increase their biocompatibility and promote cell growth. Thus, experiments showed benefits of TiO_2-modified layers, thereby opening a way to use these materials efficiently for applications in medicine, tissue engineering, and implantology.

6. List of references

1. Baranowska-Wójcik, E., et al., *Effects of titanium dioxide nanoparticles exposure on human health—a review.* Biological trace element research, 2020. **193**(1): p. 118-129.
2. Çeşmeli, S. and C. Biray Avci, *Application of titanium dioxide (TiO2) nanoparticles in cancer therapies.* Journal of drug targeting, 2019. **27**(7): p. 762-766.
3. MiarAlipour, S., et al., *TiO2/porous adsorbents: Recent advances and novel applications.* Journal of Hazardous Materials, 2018. **341**: p. 404-423.
4. Deng, J., et al., *Synthesis of Zn-doped TiO2 nano-particles using metal Ti and Zn as raw materials and application in quantum dot sensitized solar cells.* Journal of Alloys and Compounds, 2019. **791**: p. 371-379.
5. Oberbek, P., et al., *Inhalation exposure to various nanoparticles in work environment—contextual information and results of measurements.* Journal of Nanoparticle Research, 2019. **21**(11): p. 1-24.
6. Biola-Clier, M., et al., *Comparison of the DNA damage response in BEAS-2B and A549 cells exposed to titanium dioxide nanoparticles.* Mutagenesis, 2017. **32**(1): p. 161-172.
7. Brandão, F., et al., *Genotoxicity of TiO2 Nanoparticles in Four Different Human Cell Lines (A549, HEPG2, A172 and SH-SY5Y).* Nanomaterials, 2020. **10**(3): p. 412.
8. Tedja, R., et al., *Effects of serum adsorption on cellular uptake profile and consequent impact of titanium dioxide nanoparticles on human lung cell lines.* ACS nano, 2012. **6**(5): p. 4083-4093.
9. Kroll, A., et al., *Interference of engineered nanoparticles with in vitro toxicity assays.* Archives of toxicology, 2012. **86**(7): p. 1123-1136.
10. Kose, O., et al., *Impact of the Physicochemical Features of TiO2 Nanoparticles on Their In Vitro Toxicity.* Chemical research in toxicology, 2020. **33**(9): p. 2324-2337.
11. Rihova, M., et al., *Water-born 3D nanofiber mats using cost-effective centrifugal spinning: comparison with electrospinning process: a complex study.* Journal of Applied Polymer Science, 2021. **138**(5): p. 49975.
12. Bianchi, M.G., et al., *Length-dependent toxicity of TiO2 nanofibers: mitigation via shortening.* Nanotoxicology, 2020. **14**(4): p. 433-452.
13. Grigal, I.P., et al., *Correlation between bioactivity and structural properties of titanium dioxide coatings grown by atomic layer deposition.* Applied Surface Science, 2012. **258**(8): p. 3415-3419.
14. Nazarov, D.V., et al., *Enhanced osseointegrative properties of ultra-fine-grained titanium implants modified by chemical etching and atomic layer deposition.* ACS Biomaterials Science & Engineering, 2018. **4**(9): p. 3268-3281.
15. Liu, L., R. Bhatia, and T.J. Webster, *Atomic layer deposition of nano-TiO2 thin films with enhanced biocompatibility and antimicrobial activity for orthopedic implants.* International journal of nanomedicine, 2017. **12**: p. 8711-8723.
16. Kopecká, K., et al., *Exfoliation of layered mixed zirconium 4-sulfophenylphosphonate phenylphosphonates.* Dalton Transactions, 2020. **49**(12): p. 3816-3823.
17. Sopha, H., et al., *TiO2 nanotubes grown on Ti substrates with different microstructure.* Materials Research Bulletin, 2018. **103**: p. 197-204.
18. Čapek, J., et al., *Comparison of glutathione levels measured using optimized monochlorobimane assay with those from ortho-phthalaldehyde assay in intact cells.* Journal of pharmacological and toxicological methods, 2017. **88**: p. 40-45.
19. Majtnerova, P., et al., *Quantitative spectrofluorometric assay detecting nuclear condensation and fragmentation in intact cells.* Scientific reports, 2021. **11**(1): p. 11921.
20. Čapek, J. and T. Roušar, *Detection of Oxidative Stress Induced by Nanomaterials in Cells—The Roles of Reactive Oxygen Species and Glutathione.* Molecules, 2021. **26**(16): p. 4710.
21. Dawson, E., et al., *Biomaterials for stem cell differentiation.* Advanced drug delivery reviews, 2008. **60**(2): p. 215-228.
22. Park, J., et al., *Narrow window in nanoscale dependent activation of endothelial cell growth and differentiation on TiO2 nanotube surfaces.* Nano letters, 2009. **9**(9): p. 3157-3164.

7. List of student´s publications

7.1 Reports related to PhD thesis

Evaluating the use of TiO_2 nanoparticles for toxicity testing in pulmonary A549 cells. Bacova J., Knotek P., Kopecka K., Hromadko L., Capek J., Nyvltova P., Bruckova L., Schröterova L., Sestakova B., Palarcik J., Motola M., Cizkova D., Bezrouk A., Handl J., Fiala Z., Rudolf E., Bilkova Z., Macak J. M. & Rousar T. (2022). International Journal of Nanomedicine, 17, 4211-4225. DOI: 10.2147/IJN.S374955
IF: 7.033 (Q2 in Nanotechnology)

Ceramic fibers do not exhibit larger toxicity in pulmonary epithelial cells than nanoparticles of same chemical composition. Bacova J., Hromadko L., Nyvltova P., Bruckova L., Motola M., Bulanek R., Rihova M., Rousar T. & Macak J. M. (2022). Environmental Science: Nano.
DOI: 10.1039/D2EN00217E
IF: 9.473 (Q1 in Nanotechnology)

Critical comparison of aerogel TiO_2 and P25 nanopowders: Cytotoxic properties, photocatalytic activity and photoinduced antimicrobial/antibiofilm performance. Thirunavukkarasu G. K., Bacova J., Monfort O., Dworniczek E., Paluch E., Hanif M. B., Rauf S., Motlochova M., Capek J., Hensel K., Plescha G., Chodaczek G., Rousar T. & Motola M. (2022). Applied Surface Science, 579, 152145. DOI: 10.1016/j.apsusc.2021.152145
IF: 7.392 (Q2 in Materials engineering)

Removal of manganese by adsorption onto newly synthesized TiO_2-based adsorbent during drinking water treatment. Fialova K., Motlochova M., Cermakova L., Novotna K., Bacova J., Rousar T., Subrt J. & Pivokonsky M. (2021). Environmental Technology, 1-12.
DOI: 10.1080/09593330.2021.2000042
IF: 3.475 (Q3 in Earth and related environmental sciences)

Thin TiO_2 coatings by ALD enhance the cell growth on TiO_2 nanotubular and flat substrates. Motola M., Capek J., Zazpe R., Bacova J., Hromadko L., Bruckova L., Ng S., Handl J., Spotz Z., Knotek P., Baishya K., Majtnerova P., Prikryl P., Sopha H., Rousar T. & Macak J. M. (2020). ACS Applied Bio Materials, 3(9), 6447-6456. DOI: 10.1021/acsabm.0c00871
Indexed in WOSCI and Scopus.

7.2 Other published reports

The effect of repeated passaging on the susceptibility of human proximal tubular HK-2 cells to toxic compounds. Handl J., Capek J., Majtnerova P., Bacova J. & Rousar T. (2020). Physiological Research, 69(4), 731. DOI: 10.33549/physiolres.934491
IF: 2.139 (Q4 in Basic medicine)

Enantioselective synthesis of Clavaminol A, Xestoaminol C and their stereoisomers exhibiting cytotoxic activity. Novakova G., Drabina P., Bruckova L., Bacova J., Handl J., Svoboda J., Vrbicky M., Rousar T. & Sedlak M. (2020). European Journal of Organic Chemistry, 2020(24), 3671-3679. DOI: 10.1002/ejoc.202000353
IF: 3.261 (Q2 in Chemical sciences)

Influence of Cu^{2+} on osteoclast formation and activity *in vitro*. Bernhardt A., Bacova J., Gbureck U. & Gelinsky M. (2021). International Journal of Molecular Sciences, 22(5), 2451. DOI: 10.3390/ijms22052451
IF: 6.208 (Q1 in Chemical sciences)

7.3 Presentations – presenting author

Cell growth on TiO_2 nanotubes and Ti flat substrates coated with metal oxides using atomic layer deposition. Bacova J., Capek J. Sopha H., Zazpe R., Macak J.M., Rousar T. Toxcon 2022, Hradec Králové, Česká republika, 29.8.-1.9.2022, Med. Sci. Lett. (Voj. Zdrav. Listy) 2022, 91, ISSN 2571-113X.

Optimization of TiO_2 nanoparticle preparation for testing of nanotoxicity in pulmonary A549 cells. Bacova J., Majtnerova P., Knotek P., Palarcik J., Capek J., Rousar T. NANOMEET2022, Edinburgh, UK, 15.-17.8.2022.

Comparison of biological effects of inorganic fibers and nanoparticles in pulmonary cells A549. Bacova J., Hromadko L., Macak J. M., Rousar T. Bioimplantologie 2021, Mikulov, Česká republika, 7.-8.10.2021, Bioimplantologie 2021.

Assessment of potential toxicity of new synthesized nanofibers in pulmonary cells *in vitro.* Bacova J., Majtnerova P., Hromadko L., Macak J. M., Rousar T. EUROTOX 2019, 55th Congress of the European Societies of Toxicology, Helsinky, Finsko, 8.-11.9.2019, Toxicology Letters 314 (S1), str. 209 (2019), ISSN 0378-4274.

Testování toxicity nanomateriálů *in vitro*. Monitorování cizorodých látek v životním prostředí, Báčová J., Hromádko L., Macák J.M., Roušar T. Kojetín, Česká republika, 10.-12.4.2019, Sborník příspěvků ze semináře (J. Fischer, F. Božek, eds.), str. 5-13. Pardubice 2019; ISBN 978-80-7560-234-3.

7.4 Other presentations

Kometová metoda jako nástroj pro testování genotoxicity nanomateriálů. Majtnerová P., Báčová J., Macák J., Roušar T. RANK 2020, Pardubice, Česká republika, 5.-6.2.2020, Sborník RANK 2020, str. 47 (2020), ISBN 978-80-87436-17-2.

Optimalizace testování nanotoxicity *in vitro*. Roušar T., Báčová J., Brůčková L., Handl J., Majtnerová P., Čapek J., Knotek, P., Motola M.: Macák J. 96. Fyziologické dni, Martin, Slovensko, 4.-6.2.2020, Zborník abstraktov 96. Fyziologické dni Martin, str. 93, ISBN 978-80-8187-074-3.

Evaluation of the impact of TiO_2 and SiO_2 nanofibers on the neuronal cells. Handl J., Capek J., Bacova J., Hromadko L., Macak J., Rousar T. EUROTOX 2019: 55th Congress of the European Societies of Toxicology, Helsinky, Finsko, 8.-11.9., 2019, Toxicology Letters 314 (S1), str. 209 (2019), ISSN 0378-4274.

Kultivace hepatálních linií na TiO_2 materiálech. Roušar T., Brůčková L., Báčová J., Čapek J., Majtnerová P., Motola M., Macák J. XLVII. Májové hepatologické dny, Plzeň, Česká republika, 15. 17.5.2019.

Charakterizace potenciální plicní genotoxicity nanomateriálů *in vitro*. Majtnerová P., Báčová J., Macák J., Roušar T. Bioimplantologie 2019, Brno, Česká republika, 11.-12.4. 2019, Bioimplantologie 2019 (1), str. 42 (2019), ISBN 978-80-7392-307-5.

7.5 International fellowship – work experience

Practical internship focusing on research of the biological effects of bioactive ions and nanomaterials using bone cells; Center for Translational Research on Bone, Joint and Soft Tissue, Universitätsklinikum Carl Gustav Carus, Dresden, Germany; 5 months in 2020/2021.

The financial support was received from the Ministry of Education, Youth and Sports of the Czech Republic via project NANOBIO (Reg. No. CZ.02.1.01/0.0/0.0/17_048/0007421).